Boron in the Small Magellanic Cloud [1] : A Novel Test of Light Element Production

A. M. Brooks[2] and K. A. Venn[3]
Macalester College, Saint Paul, MN, 55105

D. L. Lambert
Univ. Texas Austin, Austin, TX, 78712

M. Lemke
Dr. Karl Remeis Sternwarte, Bamberg, Germany

K. Cunha[4]
Observatorio Nacional - CNPq, Rio de Janeiro, Brazil

and

V.V. Smith
Univ. Texas El Paso, El Paso, TX, 79968

ABSTRACT

Hubble Space Telescope STIS observations of the B III resonance line at 2066 Å have been obtained and analyzed for two Small Magellanic Cloud (SMC) B-type stars. While boron is not detected in either star, upper limits to the boron abundance are set, with 12+log(B/H) $\leq$ 1.6 for both AV 304 and NGC 346-637. The upper limits are consistent with the relationship between boron and oxygen previously reported for Galactic disk stars. The SMC upper limits are discussed in light of that galaxy's star formation history, present oxygen abundance, and its present cosmic ray flux.

The UV spectrum has also been used to determine the iron-group abundances in the SMC stars. For AV 304, [Fe/H]=-0.6 ± 0.2, from both an absolute and a differential analysis (with respect to the Galactic B-type star HD 36591). This is consistent with results from A-F supergiants in the SMC. A lower iron abundance is found for NGC 346-637, [Fe/H]=-1.0 ± 0.3, but this is in good agreement with the supergiant

[1]Based on observations made with the NASA/ESA *Hubble Space Telescope*, obtained at the Space Telescope Science Institute, which is operated by the Association of Universities for Research in Astronomy, Inc., under NASA contract NAS 5-26555. These observations are associated with proposal GO#07400.

[2]Columbia University, Department of Astronomy, New York, NY, 10027

[3]University of Minnesota, Department of Astronomy, Minneapolis, MN, 55455

[4]Univ. Texas El Paso, El Paso, TX, 79968

iron abundances in NGC 330, another young SMC cluster. We propose NGC 346-637 may be an unrecognized binary though, which complicates its spectral analysis.

Subject headings: abundances, Magellanic Clouds, stars:abundances, stars:evolution, stars:individual(AV 304), stars:rotation

1. Introduction

Most of the elements in the Universe have been created by either Big Bang nucleosynthesis or stellar nucleosynthesis. There are a few elements, however, that owe their existence, in part or in whole, to another site and other nuclear processes; that is, to spallation (and fusion) reactions involving galactic cosmic rays and ambient interstellar nuclei. Among this minority are lithium, beryllium, and boron (LiBeB). Understanding this trio's origins requires extensive observations of their abundances in a variety of objects. Detailed understanding of boron's nucleosynthesis has lagged behind that of the two other light elements in large part because lithium and beryllium are observable in optical spectra, but detection of boron demands UV spectroscopy. An extensive body of observational data on abundances of lithium and beryllium is available for theoretical considerations (c.f., Boesgaard *et al.* 2001, Deliyannis *et al.* 1998, Smith *et al.* 1998, and references therein), but little is presently known about boron.

Reeves, Fowler, & Hoyle (1970; with refinements by Meneguzzi, Audouze, & Reeves 1971) proposed that LiBeB are produced by spallation reactions (e.g., p + O $\rightarrow$ Li, Be, or B) and a fusion reaction ($\alpha + \alpha \rightarrow {}^6$Li and ^{7}Li) between a cosmic ray and an ambient nucleus in interstellar gas. In the local Galactic interstellar medium, the dominant contribution to the synthesis of the boron isotopes ^{10}B and ^{11}B is thought to be cosmic ray protons spallating interstellar ^{16}O nuclei. An alternative source of ^{11}B, but not ^{10}B has been proposed by Woosley *et al.* (1990); neutrino-induced spallation of ^{12}C in the carbon-burning shell of a massive star undergoing a Type II supernovae (the ν-process).

The relative contributions of galactic cosmic rays versus supernovae to boron's synthesis are ill-determined at present. A calibration of these contributions is, in principle, possible by examining the B/Be ratio, as beryllium production is not predicted by the the ν-process. Analysis of B/Be ratios are close to that predicted from spallation over a wide range of metallicities (Duncan *et al.* 1997, Garcia-Lopez *et al.* 1998). However, the uncertainties in B/Be ratios are such that a contribution ($\leq$ 30%, e.g., Lemoine *et al.* 1998, Vangioni-Flam *et al.* 1996) to ^{11}B from Type II supernovae is not excluded. Furthermore, cosmic ray spallation theory predicts the ratio ^{11}B/^{10}B = 2.5, and yet Zhai & Shaw (1994) measured a higher ratio, ^{11}B/^{10}B = 4.05, in meteorites. This result also suggests an additional contribution to the ^{11}B abundance, but it is not proof of boron synthesis in supernovae. This is because the isotopic ratio may also be increased by crafting the energy spectrum of the cosmic ray flux at the threshold energies for boron production by spallation (e.g., Meneguzzi *et al.* 1971, Prantzos *et al.* 1993, Lemoine *et al.* 1998).

To advance our understanding of the synthesis of boron, it is valuable to measure boron abundances in a diverse set of environments. Here, we describe an attempt to measure the boron abundance in the Small Magellanic Cloud, where the history of star formation, present metal abundances, and present cosmic ray flux differ from the local Galactic values. For example, in the SMC, oxygen has been well determined from both nebulae and stars, and is known to be about 1/4 as abundant as in the solar neighborhood (c.f., Korn *et al.* 2000, Hill 1999, Venn 1999, and references therein). Furthermore, Sreekumar *et al.* (1993) found that the cosmic ray flux in the SMC is no more than 1/5 that near the Sun based on EGRET observations that failed to detect γ-rays at energies $\geq$100 MeV (γ-rays are the main decay product of π^0's produced in the collision of cosmic rays with interstellar atoms).

Herein, we present boron abundances from the B III 2066 Å line from *HST* STIS spectra of two SMC main-sequence B-type stars, AV 304 and NGC 346-637. Both of these stars have been well-studied in the optical by Rolleston *et al.* (1993, 2002), so that atmospheric parameters and some elemental abundances are available. These stars show no signs of internal mixing (usually demonstrated through enrichments of surface nitrogen abundances), and Rolleston *et al.* have found oxygen abundances that are in excellent agreement with other SMC oxygen results. We have also used the *HST* STIS spectra to determine the iron-group abundances in the two SMC B-type stars, for comparison with analyses of cool SMC supergiants.

2. Target Selection and Observations

Two SMC B-type stars, AV 304 and NGC 346-637, were selected for *HST* STIS spectroscopy near the B III 2066Å line. These SMC stars are known sharp-lined objects (i.e., low $v\sin i$), which is a necessary property to be able to resolve the B III line in the crowded UV spectrum. Two main sequence B-type stars in the Galaxy (HD 36591 and HD 34078), with temperatures similar to the SMC targets (see Table 1), were also selected as standards for differential analyses.

The SMC observations (see Table 2) were made with the G230M grating (R=30,000) and a 52x0.05 slit to obtain a dispersion of 0.19 Å/pixel, or 28 km/s per resolution element. The Galactic data are from Venn *et al.* (2002 = V+02). Spectra were reduced using the STIS pipeline. The spectra were rectified using a low-order Legendre polynomial, and offset from vacuum wavelengths (observed) to air wavelengths (line list, discussed below). Additionally, the Galactic spectra were smoothed (3-pixel boxcar smoothing). The final signal-to-noise of each spectrum is listed in Table 2. The spectra are shown in Figures 1, 2, 3, and 4.

3. The Abundance Analyses

3.1. Line List

The line list and atomic data originated from the Kurucz (1988; CD-18) line list, including all lines in the the iron-group, light elements, and heavy elements lists, up to barium, and through the third ionization state. This line list was updated by including the new wavelengths for eight Fe III lines reported by Proffitt *et al.* (1999) from FTS laboratory measurements. We also updated the atomic data of 172 Fe III lines listed in Kurucz's line list by adopting the oscillator strengths and wavelengths from Ekberg (1993). This is similar to the line list used by V+02, but over a larger wavelength region (2044 to 2145Å).

Atomic data for the B III $2s^2\mathrm{S} - 2p^2\mathrm{P}$ resonance doublet with lines at 2065.8 Å and 2067.3 Å are taken from Proffitt *et al.* (1999; and discussed further by V+02). The weaker B III line at 2067.3 Å is blended with a strong Fe III line and weaker Mn III line, and is not suitable for boron abundance determinations. For all syntheses, an isotopic ratio $^{11}\mathrm{B}/^{10}\mathrm{B}= 4.0$ is assumed, the solar system ratio (Zhai & Shaw 1994, Shima 1963). This is consistent with the estimates given by Proffitt *et al.* (1999) from their line profile analyses of two sharp-lined B-type stars. Uncertainties in the use of this ratio are discussed below.

Contamination of the spectra by interstellar (IS) lines is considered. Proffitt & Quigley (2001) first noted the importance of IS lines in this wavelength range, particularly one Cr II interstellar line that can come close to the B III λ2065.8 feature depending on the stellar radial velocity. Data from Morton (1991) have been used to pinpoint the location of possible interstellar lines in the spectra and we note those that appear in all of our spectra. The SMC spectra contain doubles of each IS line, owing to more than one cloud along the line-of-sight to these stars (presumably a Galactic component and an SMC component). We have identified four IS lines; Cr II (2055.60, 2061.58, and 2065.50) and Zn II (2062.01). The locations of the IS lines are noted in the spectrum figures (see Fig.s 1 through 5). They have different locations in each figure because the spectra are shown in the stellar rest frames.

The final line list includes 6685 features between 2044 and 2145 Å. All were included in the syntheses but many are negligible contributors. A few final fine adjustments were made to the line list; after an examination of a preliminary syntheses of HD 36591, slight wavelength shifts were made to isolated strong Fe-group lines to improve the line synthesis. These fine adjustments are reported in Table 3. In addition, after the initial iron-group abundance determination was made for HD 36591 from this line list, fine adjustments were made to the oscillator strengths of five lines not previously included due to their grossly inconsistent fits in comparison to the remaining 64 lines, which are also listed in Table 3. These five lines were then included in a differential analysis. The final line list does a remarkably good job at fitting the stellar spectra over this UV range in HD 36591, AV 304, and HD 34078. This is noteworthy because UV line lists are notoriously incomplete and/or uncertain in their atomic data. Examination of the spectrum figures finds very few missing lines, and quite good fits suggesting that the energy levels and transition probabilities are fairly accurate.

3.2. Synthesizing the Spectra

Elemental abundances have been determined from LTE spectral syntheses and ATLAS9 model atmospheres (Kurucz 1979, 1988). The stellar $T_{\rm eff}$, gravity, and projected rotational velocity ($v\sin i$) values were adopted from the literature, see Table 1. The $T_{\rm eff}$ listed for HD 36591 and HD 34078 have been scaled down by 3.4% from that listed in Gies & Lambert (1992: hereafter GL92) in order to remove the increase they applied to their photometic results. Corresponding to this lower $T_{\rm eff}$, the GL92 NLTE nitrogen and oxygen abundances have been adjusted by the Δ values in their Table 9. In addition, the GL92 NLTE abundances are based on calculations made with Gold (1984) model atmospheres, instead of the more heavily line-blanketed Kurucz models. Thus, we have also applied a correction to account for the Gold-Kurucz offsets, as tabulated by Cunha & Lambert (1994, their Table 10).

Other parameters were determined from the syntheses, i.e. microturbulence (ξ) and radial velocity (as described by V+02) and are listed in Table 4. Macroturbulence (ξ_{Ma}) was initially set to the instrumental broadening values (28 km s^{-1} for the SMC stars, 15 km s^{-1} for HD 36591, and 4 km s^{-1} for HD 34078). These values were increased for the Galactic stars by 3 km s^{-1} to best fit the smoothed spectral line profiles. ATLAS9 models with 1/10 solar metallicity were used for the SMC stars, while solar metallicity models were adopted for the two Galactic stars. Spectral syntheses were made using the program LINFOR[5].

For the two cooler stars, HD 36591 (Galactic) and AV 304 (SMC), the spectrum syntheses fit the observed spectra well. For the two hotter stars, HD 34078 (Galactic) and NGC 346-637 (SMC), the initial spectrum syntheses proved to be unsatisfactory. For HD 34078, a slightly lower $v\sin i$ was required to fit its sharp line UV spectrum. Also, the preliminary iron abundance result was *very* low for a solar neighborhood object; [Fe/H]= −1.0. Since HD 34078 is one of the hottest stars analysed, then the 3.4% reduction to the GL92 temperature (discussed above) significantly affects the iron abundance[6]. Since this star is expected to have a near solar iron abundance, as it is a former member of the Orion association, then we found it is necessary to raise the temperature to 33000 K to yield this result. Accordingly, we have not completed a differential analysis of NGC 346-637 with respect to HD 34078 because of the uncertainties in the parameters of this hot star. However, HD 34078 is included in Figs 1 through 4 to show the high quality of our line list, even at hot temperatures.

The analysis of NGC 346-637 also had some difficulties, beginning with its radial velocity.

---

[5]LINFOR was originally developed by H. Holweger, W. Steffen, and W. Steenbock at Kiel University. It has been upgraded and maintained by M. Lemke, with additional modifications by N. Przybilla.

[6]Note that this iron-group abundance result is also lower than that reported by V+02 for HD 34078 for two reasons. Firstly, V+02 synthesized fewer features (twelve in 22 Å, whereas 25 features are synthesized over 70 Å in this paper). Secondly, the iron abundance is *very* sensitive to temperature in *hot* stars (see the temperature sensitivities listed in Table 7 of V+02). The 3.4% temperature effect on abundances was applied to the boron and CNO abundances in the discussion by V+02, but not to iron since it was an insignificant effect for the stars in the discussion in that analysis.

We found that a radial velocity of 250 km s^{-1} was necessary to best fit the *HST* STIS data, yet Rolleston *et al.* (1993) reported a value of ∼100 km s^{-1} for this star. A large radial velocity is unusual; the velocities for SMC stars tends to range from 100 − 180 km s^{-1} (e.g., Venn 1999, Rolleston *et al.* 1993, Grebel *et al.* 1996). In addition, the spectrum synthesis proved to be quite difficult, with very few clean iron-group lines available to constrain the fitting parameters (see Figs. 1 to 4). An SMC-like iron-group abundance (discussed below) was found, [Fe/H] = −1.0 ±0.3 (see Table 5), but our spectrum fits were not very satisfactory. We examined other spectrum syntheses over a range in atmospheric parameters (i.e., $T_{\rm eff}$, gravity, radial velocity, and $v\sin i$), but no significant improvements were found. We suspect that this star may be an unresolved binary. Binarity could explain the large and, apparently, variable radial velocity for this star, and could affect the spectrum synthesis if the companion contributes continuum to the UV spectrum.

3.3. Iron-group & Synthesis Parameters

The iron-group abundances were determined from synthesis of specific features in the spectra and results from the individual features were averaged. In Table 5, the line abundances are listed relative to the meteoritic abundances from Grevesse & Sauval (1998), e.g. log(Fe)= 7.50 and log(Mn)= 5.53. The mean abundances in Table 5 were calculated by excluding line abundances that fall more than 2σ from the mean (of the line-to-line scatter).

We estimate an uncertainty of approximately ±2 km s^{-1} in the macroturbulence, based on line profile fitting, but only ±1 km s^{-1} in microturbulence based on line strengths. Iron-group uncertainties for HD 36591 and HD 34078 were previously determined by V+02. These uncertainties are adopted here for the SMC stars since the atmospheric parameters and analysis method are similar. NLTE effects are neglected throughout this iron-group analysis. Iron-group abundances are determined primarily from lines of the dominant ionization species of the elements, i.e., Fe III.

As expected, near solar mean iron-group abundances are found for HD 36951, [Fe/H]=−0.07 ±0.10 from 46 features. The iron-group abundance for AV 304 is [Fe/H]=−0.6 ±0.2 from 24 features, which is identical to a differential line-by-line comparison with HD 36591 (including the five additional features with altered oscillator strengths discussed above for a total of 29 lines). This metallicity is similar to Rolleston *et al.'s* (1993) results for AV 304's light elements (e.g. Si, Mg), as well as a pioneering attempt to determine iron in AV 304 based on GHRS spectra by Peters & Grigsby (1999). It is also in good agreement with iron abundances in cooler supergiants ($-1.0 <$ [Fe/H] < -0.5; Venn 1999, Hill 1999, 1997, Luck *et al.* 1998, Russell & Bessell 1989).

The mean iron-group abundance for NGC 346-637 is [Fe/H]= −1.0 ±0.3, determined from nine features. A differential analysis of these nine features, plus three more with corrected oscillator strengths, with respect to the cooler Galactic star HD 36591 yields −1.0 ±0.4 dex (recall, due to uncertainties in $T_{\rm eff}$ for HD 34078, we do not present a differential analysis of

NGC 346-637 with this star even though they are both hotter stars). The iron-group abundance for NGC 346-637 is somewhat lower than that for AV 304, which could be explained by dilution of the UV continuum by a companion if NGC 346-637 is an unrecognized binary (discussed above). However, NGC 346-637 has an iron abundance that is within the range of the results from young supergiants, and it is in excellent agreement with the iron abundance found for supergiants in the young SMC cluster NGC 330 (Hill 1999, Luck *et al.* 1998).

3.4. Boron Abundances

LTE boron abundances for the SMC stars are listed in Table 4 following the procedures detailed by Venn *et al.* (2002). The spectrum synthesis for HD 36591 is slightly different from that in V+02 because $T_{\rm eff}$ has been lowered 3.4% from the GL92 here; also, the temperature for HD 34078 is higher, 33,000 K, to yield solar-like abundances (discussed above).

In general, no attempt was made to constrain the weak Mn III λ2065.9 line abundance *a priori*, which is blended with the B III λ2065.8 feature, as described by V+02. However, in the case of AV 304, an unfortunate noise spike redward of the boron feature causes the Mn III abundance to be indeterminate. Therefore, we have adopted the underabundance suggested by the iron-group analysis. In the analysis by V+02, it was found that the Mn III 2065.9 line abundance was generally in good agreement with the iron-group determination, with $-0.3 \geq$ [Mn/Fe] ≤ -0.05. If [Mn/Fe] $= -0.3$, it does not alter the boron upper limit for AV 304. The iron-group abundance was also adopted for the Mn III 2065.9Å line in NGC 346-637 and HD 34078 as this feature seems to be insignificant at these hotter temperatures (i.e. lowering the Mn III abundance further does not alter our boron upper limits).

As noted above, an isotopic ratio of ^{11}B/^{10}B = 4.0 is adopted. Of course, this ratio is undetermined in the SMC, and a purely GCR spallation model predicts ^{11}B/^{10}B = 2.5. Calculations show that the difference in the boron abundance yielded by using a ratio of 2.5 or 4.0 is negligible, $\Delta\log({\rm B/H}) \leq 0.05$ for both SMC stars.

To compute the boron abundance *uncertainties* independent of uncertainties in Mn III λ2065.9, it was found necessary to fix the Mn III line abundance *a priori*. The Mn III line abundance was set to the best fit value (in Table 4). A second method of setting the Mn III abundance according to the Fe-group uncertainties for each parameter was examined by V+02 and found to yield similar boron uncertainties. Table 6 shows that the most significant uncertainty in the boron abundances tends to be the continuum placement (thus, S/N of the data). The two hottest stars, HD 34078 and NGC 346-637, are also sensitive to the atmospheric parameters, particularly $T_{\rm eff}$. In general, hot stars are not the best boron indicators. While the result for NGC 346-637 is consistent with a lower boron abundance in the SMC, it is possible that *no* boron exists in NGC 346-637 to within the errors caused by the low signal-to-noise spectrum. This is shown in Fig. 5, where the best fit upper limit is shown, with +0.3 and 12+log(B/H) $= -10$ for

comparison. Finally, in Table 4, the LTE boron abundances are corrected for NLTE effects using calculations reported in V+02.

4. Discussion

4.1. Boron and Oxygen in the SMC and the Galaxy

Boron synthesis, whether controlled by spallation in the interstellar medium or by Type II supernovae, is coupled to the growth of the oxygen abundance. Therefore, it is of interest to establish the relationship between boron and oxygen in the SMC.

At present, our boron upper limits in two young stars are the sole data points on boron ($12 + \log(\mathrm{B/H}) \leq 1.6$ in both). The oxygen abundances in our SMC targets are listed in Table 1, and are in excellent agreement with oxygen results from other young SMC stars and H II regions. Oxygen abundances in the SMC have been determined from H II regions, hot and cool supergiants, and B-type main sequence stars. The results are pleasingly consistent - see summary by Venn (1999, Table 9). More recent results include additional analyses of B-type stars by Korn *et al.* (2000) and Dufton *et al.* (2000), who found mean abundances $12 + \log(\mathrm{O/H}) = 8.15$ and 8.0, respectively.

A comparison of boron and oxygen can also be made for Galactic stars and the local interstellar medium. In Table 7, we list boron abundances in local Pop. I stars and nebulae, and adopt $12 + \log(\mathrm{B/H}) = 2.5$ in the solar neighborhood. Furthermore, we adopt $12 + \log(\mathrm{O/H}) = 8.7$ (see Allende Prieto *et al.* 2001) for the present local oxygen abundance. Additional local boron abundances have been determined over a wide range in metallicities, and several studies have reported on the boron-oxygen correlation (e.g., Garcia-Lopez *et al.* 1998, Duncan *et al.* 1997). Smith, Cunha, & King (2001) provide a reassessment of the relation between boron and oxygen in Galactic F- and G-type dwarfs. The oxygen abundances in stars where the B I 2497 Å line was observed led to a correlation represented by $\mathrm{B/H} \propto (\mathrm{O/H})^m$ with $m = 1.4 \pm 0.1$ for stars with $-0.4 < [\mathrm{O/H}] < +0.2$, see Fig. 6. (Note that our adopted initial local Galactic abundances for boron and oxygen lay on this line in Fig. 6). On including results from the literature to extend the relation to lower metallicities, Smith *et al.* found $m \simeq 1.0$ or 1.4 for stars with $[\mathrm{Fe/H}] \leq -1.0$ depending on the adopted set of oxygen abundances in the metal-poor stars. The uncertainties in oxygen in metal-poor stars is an ongoing debate at present (c.f., Lambert 2001). Also, it should be noted that the abundances of beryllium, a product solely of spallation, behave in a very similar way to boron, and the B/Be ratio is approximately constant from solar metallicity stars to the most metal-poor (Boesgaard *et al.* 1999).

In Fig. 6, we show the oxygen abundances and boron upper limits established for the two SMC stars reported here. The solid line is the Smith *et al.* fit to the B–O relation for the Galactic stars with B α $\mathrm{O}^{1.4}$, while the dashed lines indicate linear and quadratic trends of B with O. If taken at face value, the results for the two SMC stars would suggest that the boron-oxygen

relationship in the SMC is in excellent agreement with that of the Galactic disk.

4.2. Boron Depletion Mechanisms

A discussion of boron synthesis in the SMC assumes that boron has not been depleted in the stellar atmosphere, and should represent the present day abundance in the interstellar medium. Observations of Galactic B-type stars, however, show that boron depletion is not uncommon (Venn *et al.* 2002, Proffitt & Quigley 2001). Therefore, the possibility of loss of atmospheric boron must be recognized.

Several processes are capable of reducing the boron abundance while a B-type star is on the main sequence. The most likely process is rotationally-induced mixing, although mass loss, or mass transfer from an evolved companion, would also produce the same result. Mass loss from *main sequence* B-type stars is not expected to have a significant effect on the surface B abundance (see the discussion in Fliegner *et al.* 1996, and V+02). It would require a mass loss rate an order of magnitude larger than observed for Galactic B-type stars (Cassinelli *et al.* 1994). For SMC stars, we expect the winds to be even weaker since winds of hot stars are driven by photon momentum transfer through metal line absorption, thus a function of metallicity (c.f., Kudritzki & Puls 2000).

Mass transfer in a close binary system will not affect boron in the mass-receiving (i.e., the observed) star without a considerable enrichment of nitrogen (c.f., Wellstein 2000). For AV 304, Rolleston *et al.* (2002) find the nitrogen abundance $12 + \log(\mathrm{N/H}) = 6.7 \pm 0.2$ from N II lines measured from a VLT UVES spectrum. The fact that this abundance is in very good agreement with those measured in SMC H II regions (Dufour 1984; Russell & Dopita 1990; Kurt *et al.* 1999), and for other B-type stars (e.g., Korn *et al.* 2000) eliminates the idea that mass transfer could have affected its boron abundance. For NGC 346-637, the picture is unclear. Rolleston *et al.* (1993) could determine only an upper limit to the nitrogen abundance: $12 + \log(\mathrm{N/H}) \leq 7.2$, which does not entirely exclude the possibility that mass transfer may have affected the surface abundances. Furthermore, we suspect this star may be an unrecognized binary (see Section 3.2).

Depletion of boron by rotationally-induced mixing cannot be ruled out. Recent models by Heger & Langer (2000) follow the evolution of the angular momentum distribution in intermediate-mass stars from the pre-main sequence through core collapse, and find that rotational mixing can affect stellar surface abundances of boron and nitrogen. For rapidly rotating stars, boron can be depleted and nitrogen enriched at the surface. V+02 have confirmed that these models do indeed fit the observed abundances of boron and nitrogen in Galactic B-type stars. Boron is predicted to be depleted ahead of detectable nitrogen enrichment. While nitrogen-rich stars are predicted and observed to be boron depleted (Proffitt & Quigley 2001, V+02), stars showing a normal nitrogen abundance may also be boron depleted by as much as 1 dex! Thus, this is a possibility which we cannot exclude for either AV 304 or NGC 346-637. To reduce this possibility additional stars would have to be observed to search for stars with a higher boron

abundance. (While lithium and beryllium would be depleted too, these elements are not observable in B-type stars.)

4.3. Spallation in the SMC

In the case of the solar neighborhood, the contribution of spallation to the synthesis of boron is assessable from measurements of the beryllium abundance in stars; beryllium owes its origins exclusively to spallation and the B/Be ratio is predictable with fair certainty. Unfortunately, there are no determinations of the Be abundance in SMC gas or stars, and one must predict the production rate of boron from the ingredients controlling it.

Suppose boron is produced by the process p_{CR}+O$_{ISM}$ $\rightarrow$ B, the production rate dn_B/dt involves three factors: the cosmic ray proton flux (ϕ_{CR}), the O abundance in the interstellar medium ($n(O)$), and the spallation cross-section ($\sigma(O \rightarrow B)$), that is

$$\frac{dn_B}{dt} = \phi_{CR} n(O) \sigma(O \rightarrow B) \quad (1)$$

where the energy dependences of the factors are suppressed and an integral over energy is implicit. To this rate must be added contributions from C and N as targets, and from α-particles as projectiles.

The production rate at present in the SMC would appear to be much less than that in the local regions of the Galaxy because (i) the oxygen abundance (n(O)) in the SMC is a factor of 4 lower than in the local interstellar medium (see Section 4.1), and (ii) the upper limit on the cosmic ray flux in the SMC is at least a factor of 5 less than the local flux (Sreekumar *et al.* 1993). Taken together, $\frac{dn_B}{dt}$ for the SMC could be a factor of 20 less than the local rate. But the boron abundance at a given time and location is an integral of the production rate; a low rate now does not of itself preclude higher rates in the past. Thus, the history of the cosmic ray flux can also contribute to predicting the boron abundance.

4.3.1. History of the Cosmic Ray Flux

The history of the cosmic ray flux (=CRF) must be known in order to calculate the evolution of the boron abundance. The confinement time of Galactic cosmic rays is short (below), and, hence, the present flux is no guide to the past flux of cosmic rays. Measurements of the abundance of secondary fragments produced in the interstellar medium by nuclear interactions between cosmic rays and ambient nuclei have provided estimates of the confinement time for Galactic cosmic rays. Radioctive ^{10}Be was the first 'clock' to be proposed (Hayakawa *et al.* 1958). Now, measurements of ^{10}Be, ^{26}Al, ^{36}Cl, and ^{54}Mn all indicate a confinement time of about 15 Myr (Yanasak *et al.* 2001). Clearly, galactic cosmic rays must be continuously replenished if spallation is to work its magic.

The confinement time for the SMC is probably shorter. The magnetic field lines of the SMC are expected to be highly disrupted due to interactions with the Galaxy and the LMC. Mathewson (1986, 1988) and Murai & Fujimoto (1980) suggest that a close encounter between the Magellanic Clouds and the Milky Way occurred about 200 Myr ago, and observations show it is likely that this disturbance disrupted the magnetic field lines of the SMC (Wayte 1990; Haynes *et al.* 1991; Ye & Turtle 1991; Goldman 2000). As cosmic rays are highly ionized particles, they are generally trapped by the magnetic field lines within a galaxy; thus, disrupted magnetic field lines in the SMC may lead to shorter lifetimes for cosmic rays in the SMC.

Thus, the present CRF in the SMC is not likely to be the same as in the past. For example, a large burst of star formation that began 2-4 Gyr ago enriched the SMC to its present oxygen abundance (e.g., Pagel & Tautvaisiene 1998, Mighell *et al.* 1998, de Freitas Pacheco *et al.* 1998, Gardiner 1992), and it should also have produced a higher CRF. However, the star formation rate is thought to have declined since that time, and hence the CRF could also have declined. We expect the present low flux is a recent phenomenon that should have no influence on the boron-oxygen correlation.

4.3.2. Boron vs Oxygen Relationship

Although the source of the cosmic rays and the identity of the acceleration mechanism are uncertain, it is assumed that the CRF is linked to the presence of supernovae. Thus, given the short confinement time, $\phi_{CR} \propto N_{SN}(t)$ is a plausible approximation. Since oxygen is a product of Type II supernovae, one may suppose that $dN_{SN}/dt \propto dn(O)/dt$. If it is assumed that the constant of proportionality between the CRF and the number of supernovae is time independent, equation (1) predicts that $\mathrm{B/H} \propto (\mathrm{O/H})^m$ with $m \equiv 2$. This result does not depend on an assumption of a time-independent dn_B/dt; star formation in bursts (as in the SMC) does not necessarily invalidate the result. As long as the mean lifetime of the cosmic rays is short relative to the durations of the burst and the CRF is tied to that of the O-producing massive stars, the production rate integrated over time will result in the quadratic dependence.

Direct comparison of the boron vs oxygen relationship in the Galaxy and the SMC will be inappropriate if the efficiency of cosmic ray generation in supernovae is different for the two galaxies. Nonetheless, it is of interest to make such a comparison. In the solar neighborhood, we adopt $12 + \log(\mathrm{B/H}) = 2.5$ and $12 + \log(\mathrm{O/H}) = 8.7$ (see Section 4.1). Adopting $12 + \log(\mathrm{O/H}) = 8.1$ for the SMC, the quadratic relation predicts $12 + \log(\mathrm{B/H}) = 1.3$ for the SMC, a value that is 0.3 dex below our measured upper limits. If cosmic rays do escape more easily from the SMC (discussed above), then the boron production rate per oxygen atom produced by supernovae would be smaller in the SMC. Recognition of this fact would result in a predicted boron abundance that is even lower than $12 + \log(\mathrm{B/H}) = 1.3$.

While our boron upper limits are in fair agreement with the quadratic prediction, the quadratic

approximation is of questionable validity, at least for the solar neighborhood. Observations of boron and oxygen abundances in stars for which boron is undepleted do *not* show the quadratic dependence (see Section 4.1): as noted, $m = 1.4$ for Galactic stars of approximately solar metallicity, and a lower index (e.g., $m \simeq 1$) may be required to fit the observations of metal-poor stars (Smith *et al.* 2001). If $m = 1.4$ is adopted, the predicted SMC boron abundance ($12 + \log(\mathrm{B/H}) \sim 1.6$) is in excellent agreement with our upper limits. An index $m = 1$ predicts a boron abundance 0.3 dex greater than our upper limits for the SMC stars. While a difference of 0.3 dex is within 3 σ of our boron upper-limits, we note that this agreement worsens for our best analysed star, AV 304. For AV 304, $12 + \log(\mathrm{O/H}) = 8.2$, thus a slope of $m = 1$ predicts a boron abundance that is 0.4 dex larger than our upper limit. This result argues against a purely linear relation between oxygen and boron in the SMC, unless we need to consider rotationally induced depletion, and/or the possibility of less efficient production and/or retention of cosmic rays in the SMC.

Other schemes may also be devised that allow for values of m less than 2. In the context of spallation, a simple way is to consider the 'reverse' of the 'direct' process introduced above. For the reverse reaction $\mathrm{O}_{CR} + p_{ISM} \rightarrow \mathrm{B}$, and a boron-oxygen relation with $m = 1$, that is $\mathrm{B} \propto \mathrm{O}$ is expected. The reverse rate is often neglected because it produces higher velocity boron nuclei than the direct process, and the losses before the nuclei are thermalized are greater than for directly produced boron. Furthermore, when the interstellar medium has approximately solar abundances of C, N, and O, the reverse process is much less effective than the direct process. For example, in the early Galaxy, the oxygen abundance in the interstellar medium was lower, but the cosmic rays, if they were accelerated material from supernova ejecta, may have had a similar oxygen abundance to contemporary cosmic rays. This circumstance would favor the reverse rate. In the limit that the reverse process was dominant at low metallicities, one expects a switch from $m = 1$ to $m = 2$ as O/H increases in simple galactic models. And, in fact, depending on the choice for the oxygen abundances in metal-poor stars, there is a trend from $m \simeq 1$ at low metallicity to a higher value ($m = 1.4$) at solar metallicity (see Smith *et al.* 2001).

Finally, two other scenarios may be mentioned. First, if cosmic rays are not of galactic origin, their flux would be independent of the supernova rate, which would affect all boron-oxygen relations. However, there is ample evidence that the extragalactic component to Galactic cosmic rays is small (e.g., Pannuti 2000, Dickel 1974, Butt *et al.* 2001), including the fact that the SMC does not have the same CRF as seen in the local Galaxy (Sreekumar *et al.* 1993). Second, if boron is primarily a product of neutrino-induced spallation in Type II supernovae, then one expects $m \simeq 1$. However, the contribution by this process is currently estimated at $\leq 30\%$ in the Galaxy (e.g., Lemoine *et al.* 1998, Vangioni-Flam *et al.* 1996).

5. Conclusions

We have analysed *HST* STIS observations of the B III resonance line at 2066 Å for two SMC B-type stars. The upper limits corrected for small non-LTE effects are $12 = \log(\mathrm{B/H}) \leq 1.6$ for

both AV 304 and NGC 346-637. Unless the stars have internally depleted boron by a large factor, we show that the upper limits are plausibly consistent with the hypothesis that boron is a product of spallation induced by cosmic rays. Significant production by neutrino-induced spallation of ^{12}C in Type II supernovae is probably excluded unless the initial boron abundance was a factor of 2 higher than our upper limits.

The UV line list is quite excellent for spectrum synthesis at Galactic and SMC metallicity in this temperature range. For AV 304, we find [Fe/H]=-0.6 ± 0.2 from both an absolute and differential analysis with HD 36591. This is consistent with results from the A-F supergiants in the SMC. In comparison, the fewer and weaker iron-group lines in the spectrum of NGC 346-637 result in a less certain abundance, [Fe/H]=-1.0 ± 0.3. We also suggest that this star may be an unresolved binary.

Support for proposal GO#08161 was provided by NASA through a grant from the Space Telescope Science Institute, which is operated by the Association of Universities for Research in Astronomy, Inc., under NASA contract NAS 5-26555. KAV and AB acknowledge additional research support from Macalester College and the Luce Foundation through a Clare Boothe Luce Professorship award. We would like thank Grace Mitchell (STScI) for expertise in reducing the STIS data.

REFERENCES

Ahlen, S.P., Greene, N.R., Loomba, D., Mitchell, J.W., Bower, C.R., Heinz, R.M., Mufson, S.L., Musser, J., Pitts, J.J., Spiczak, G.M., Clem, J., Guzik, T.G., Lijowski, M., Wefel, J.P., McKee, S., Nutter, S., Tomasch, A., Beatty, J.J., Ficenec, D., Tobias, S., 2000, ApJ, 534, 757

Allende Prieto, C., Lambert, D.L., Asplund, M., 2001, ApJ, 556, 63

Anders, E., Grevesse, N., 1989, *GeoChim.CosmoChim.*, 53, 197

Audouze, J., Reeves, H., 1982, in *Essays in Nuclear Astrophysics*, ed. C.A. Barnes, D.D. Clayton, & D.N. Schramm (Cambridge: Cambridge Univ. Press), 355

Austin, S.M., 1981, Prog. Particle Nucl. Phys., Vol. 7, 1

Barbuy, B., 1988, A&A, 191, 121

Bloemen, H., Morris, D., Knödlseder, J., Bennet, K., Diehl, R., Hermsen, W., Lichti, G., van der Meulen, R.D., Oberlack, U., Ryan, J., Schönfelder, V., Strong, A.W., de Vries, C., Winkler, C., 1999, ApJ, 521, 2, L137

Bloemen, H., Wijnands, R., Bennet, K., Diehl, R., Hermsen, W., Lichti, G., Morris, D., Ryan, J., Schönfelder, V., Strong, A.W., Swanenburg, B.N., de Vries, C., Winkler, C., 1994, A&A, 281, 1, L5

Boesgaard, A.M., Deliyannis, C.P., King, J.R., Stephens, A., 2001, ApJ, 553, 754

Boesgaard, A.M., Deliyannis, C.P., King, J.R., Ryan, S.G., Vogt, S.S., Beers, T.C., 1999, AJ, 117, 1549

Butt, Y.M., Torres, D.F., Combi, J.A., Dame, T., Romero, G.E., ApJLett., 562, L167

Cassé, M., Lehoucq, R., Vangioni-Flam, E., 1995, Nature, 373, 318

Connell, J.J., 1998, ApJLet., 501, 59

Cunha, K., Lambert, D.L., 1992, ApJ, 399, 586

Cunha, K., Lambert, D.L., 1994, ApJ, 426, 170 (=CL94)

Cunha, K., Lambert, D.L., Lemke, M., Gies, D.R., Roberts, L.C., 1997, ApJ, 478, 211

Cunha, K., Smith, V.V., 1999, ApJ, 512, 1006

Cunha, K., Smith, V.V., Lambert, D.L., 1999, ApJ, 519, 844

Cunha, K., Smith, V.V., Boesgaard, A., Lambert, D.L., 2000a, ApJ, 530, 939

Cunha, K., Smith, V.V., Parizot, E., Lambert, D.L., 2000b, ApJ, 543, 850

Daflon, S., Cunha, K., Becker, S.R., Smith, V.V., 2001, ApJ, 552, 309

Delbourgo-Salvador, P., Vangioni-Flam, E., 1993, in Origin and Evolution of the Elements, ed. N. Prantzos *et al.* (Cambridge: Cambridge Univ. Press), 132

Deliyannis, C.P., Boesgaard, A.M., Stephens, A., King, J.R., Vogt, S.S., Keane, M.J., 1998, ApJ, 498, 147

Dickel, J.R., 1974, ApJ, 193, 755

Dufour, R.J., 1984, in IAU Symp. 108, Structure and Evolution of the Magellanic Clouds, ed. S. van den Bergh & K.S. de Boer (Dordrecht: Reidel), 353

Dufton, P.L., McErlean, N.D., Lennon, D.J., Ryans, R.S.I., 2000, A&A, 353, 311

Duncan, D.K., Lambert, D.L., Lemke, M., 1992, ApJ, 401, 584

Duncan, D.K., Primas, F., Rebull, L.M., Boesgaard, A.M., Delyannis, C.P., Hobbs, L.M., King, J.R., Ryan, S.G., 1997, ApJ, 488, 338

Ekberg, J.O., 1993, A&AS, 101, 1 (=E93)

Fields, B.D., Olive, K.A., 1999, ApJ, 516, 797

Fulbright, J.P., Kraft, R.P., 1999, AJ, 118, 527

Garcia Lopez, R.J., 2000, IAU joint discussion 8, Manchester, UK.

Garcia Lopez, R.J., Lambert, D.L., Edvardsson, B., Gustafsson, B., Kiselman, D., Rebolo, R., 1998, ApJ, 500, 241

Gies, D.R., Lambert, D.L., 1992, ApJ, 387, 673 (=GL92)

Gold, M., 1984, Ph.D. thesis, Diplomarbeit Univ. München

Goldman, I., 2000, ApJ, 541, 701

Gratton, R.G., Ortolani, S., 1989, A&A, 211, 41

Grebel, E.K., Roberts, W.J., Brandner, W., 1996, A&A, 311, 470

Grevesse, N., Sauval, A.J., 1998, Space Sci. Rev., 85, 161

Gummersbach, C.A., Kaufer, A., Schäfer, D.R., Szeifert, T., Wolf, B., 1998, A&A, 338, 881

Hayakawa, S., Ito, K., Terashima, Y., 1958, Prog. Theor. Phys. Suppl., 6, 1

Haynes, R.F., Klein, U., Wayte, S.R., Wielebinski, R., Murray, J.D., Bajaja, E., Meinert, D., Buczilowski, U.R., Harnett, J.I., Hunt, A.J., Wark, R., Sciacca, L., 1991, A&A, 252, 475

Heger, A., Langer, N., 2000, ApJ, 544, 1016

Hill, V., 1999, A&A, 345, 430

Hill, V., 1997, A&A, 324, 435

Hill, V., Barbuy, B., Spite, M., 1997, A&A, 323, 461

Howk, J.C., Sembach, K.R., Savage, B.D., 2000, ApJ, 543, 278

Israelian, G., Garcia Lopez, R.J., Rebolo, R., 1998, ApJ, 507, 805

Jura, M., Meyer, D.M., Hawkins, I., Cardelli, J.A., 1996, ApJ, 456,598

Kilian-Montenbruck, J., Gehren, T., Nisenn, P.E., 1994, A&A, 291, 757

King, J.R., 2000, AJ, 120, 1056

Korn, A.J., Becker, S.R., Gummersbach, C.A., Wolf, B., 2000, A&A, 353, 655

Kraft, R.P., Sneden, C., Langer, G.E., Prosser, C.F., 1992, AJ, 104, 645

Kraft, R.P., Sneden, C., Langer, G.E., Shetrone, M.D., Bolte, M., 1995, AJ, 109, 2586

Kraft, R.P., Sneden, C., Smith, G.H., Shetron, M.D., Langer, G.E., Pilachowski, C.A., 1997, AJ, 113, 279

Kudritzki, R.P., Puls, J. 2000, ARAA, 38, 613

Kurt, C.M., Dufour, R.J., Garnett, D.R., Skillman, E.D., Mathis, J.S., Peimbert, M., Torres-Peimbert, S., Ruiz, M.-T., 1999, ApJ, 518, 246

Kurucz, R.L., 1979, ApJS, 40, 1

Kurucz, R.L., 1988, Trans. IAU, Vol. 20B, ed. M. McNally (Dordrecht: Kluwer)

Lambert, D.L., 2001, in IAU Joint Discussion, Oxygen Abundances in Old Stars and Implications to Nucleosynthesis and Cosmology, ed. B. Barbuy (Dordrecht: IAU), in press

Lambert, D.L., Sheffer, Y., Federman, S.R., Cardelli, J.A., Sofia, U.J., Knauth, D.C., 1998, ApJ, 494, 614

Lemke, M., Cunha, K., Lambert,D.L., 2000, in *The Galactic Halo: From Globular Cluster to Field Stars*, Proc. of the 35th Liege International Astrophysics Colloquium, eds. A. Noels, P. Magain, D. Caro, E. Jehin, G. Parmentier, and A. A. Thoul. (Liege: Institut d'Astrophysique et de Geophysique), p.223

Lemoine, M., Vangioni-Flam, E., Cassé, M., 1998, ApJ, 499, 735

Luck, R.E., Moffett, T.J., Barnes, T.G., Gieren, W.P., 1998, AJ, 115, 605

Lukasiak, A., Ferrando, P., McDonald, F.B., Webber, W.R., 1994, ApJ, 423, 426

Mathewson, D.S., Ford, V.L., Visvanathan, N., 1986, ApJ, 301, 664

Mathewson, D.S., Ford, V.L., Visvanathan, N., 1988, ApJ, 333, 617

Meneguzzi, M., Audouze, J., Reeves, H., 1971, A&A, 15, 337

Mighell, K.J., Sarajedini, A., French, R.S., 1998, AJ, 116, 2395

Morton, D.C., 1991, ApJS, 77, 119

Murai, T., Fujimoto, M., 1980, PASP, 32, 581

Pagel, B.E.J., Tautvaisiene, G., 1998, MNRAS, 299, 535

Pannuti, T.G., 2000 *Ph.D. thesis*, U. New Mexico.

Parizot, E., Cassé, M., Vangioni-Flam, E., 1997 A&A, 328, 107

Pavlidou, V., Fields, B.D., 2001, ApJ, submitted

Peters, G.J., Grigsby, J.A., 1999, AAS, 195, 50.09

Pinsonneault, M., 1997, ARAA, 35, 557

Prantzos, N., Cassé, M., Vangioni-Flam, E., 1993, ApJ, 403, 630

Primas, F., Duncan, D.K., Peterson, R.C., Thorburn, J.A., 1999, A&A, 343 545

Proffitt, C.R., Jönsson, P., Pickering, J.C., Wahlgren, G.M., 1999, ApJ, 516, 342

Proffitt, C.R., Quigley, M.F., 2001, ApJ, 548, 429

Ramaty, R., Kozlovsky, B., Lingenfelter, R.E., 1996, ApJ, 456, 525

Reeves, H., Fowler, W.A., Hoyle, F., 1970, Nature, 226, 727

Rolleston, W.R.J., Dufton, P.L., Fitzsimmons, A., Howarth, I.D., Irwin, M.J., 1993, A&A, 277, 10 (=R+93)

Rolleston, W.R.J., Venn, K.A., *et al.* , 2002, in prep. (=R+02)

Russell, S.C., Dopita, M.A., 1990, ApJS, 74, 93

Russell, S.C., Bessell, M.S., 1989, ApJS, 70, 865

Shima, M., 1963, Geochim. Cosmochim. Acta, 27, 991

Simpson, J.A., Garcia-Munoz, M., 1988, Space Sci. Rev, Vol.46, No.3-4, p.205

Smartt, S.J., Rolleston, W.R.J., 1997, ApJLet., 481, 47

Smith, V.V., Lambert, D.L., Nissen, P.E., 1998, ApJ, 506, 405

Sneden, C., Kraft, R.P., Prosser, C.F., Langer, G.E., 1991, AJ, 102, 2001

Spite, M., Spite, F., 1985, ARAA, 23, 225

Sreekumar, P., Bertsch, D.L., Dingus, B.L., Fitchel, C.E., Hartman, R.C., Hunter, S.D., Kanbach, G., Kniffen, D.A., Lin, Y.C., Mattox, J.R., Mayer-Hasselwander, H.A., Michelson, P.F., von Montigny, C., Nolan, P.L., Pinkau, K., Schneid, E.J., Stone, R.G., Thompson, D.J., 1993, Phys. Rev. Letts., 70, 127

Sreekumar, P., Fitchel, C., 1991, A&A, 251, 447

Stasińska, G., Richer, M.G., McCall, M.L., 1998, A&A, 336, 667

Thomas, D., Schramm, D.N., Olive, K.A., Fields, B.D., 1993, ApJ, 406, 569

Timmes, F.X., Woosley, S.E., Weaver, T.A., 1995, ApJS, 98, 617

Vangioni-Flam, E., Cassé, M., Fields, B.D., Olive, K.A., 1996, ApJ, 468, 199

Venn, K.A., 1999, ApJ, 518, 405

Venn, K.A., Brooks, A.M., Lambert, D.L., Lemke, M., Langer, N., Lennon, D.J., Keenan, F.P., 2001, ApJ, in press (=V+02)

Venn, K.A., Lambert, D.L., Lemke, M., 1996, A&A, 307, 849

Vrancken, M., Lennon, D.J., Dufton, P.L., Lambert, D.L., 2000, A&A, 358, 639

Wayte, S.R., 1990, ApJ, 355, 473

Webber, W.R., Soutoul, A., 1998, ApJ, 506, 335

Wellstein, S., 2001, *Ph.D. thesis*, U. Potsdam.

Wheeler, J.C., Sneden, C., Truran, J.W., Jr., 1989, in ARA&A, Vol.27, p.279

Woosley, S.E., Hartmann, D.H., Hoffmann, R.D., Haxton, W.C., 1990, ApJ, 356, 272

Ye, T., Turtle, A.J., 1991, MNRAS, 249, 722

Yanasak, N.E., *et al.* , 2001, Adv. Space Res., 27, 727

Yoshii, Y., Kajino, T., Ryan, S.G., 1997, ApJ, 485, 605

Zhai, M., Shaw, D.M., 1994, Meteoritics, 29, 607

Table 1. Atmospheric Parameters from the Literature

Star	SpType	$T_{\rm eff}$ (K)	log g	$v \sin i$ (km s^{-1})	12+log(O/H) (NLTE)	12+log(N/H) (NLTE)	REF
HD 36591	B1IV	26449	4.15	11	8.67 ±0.22	7.69 ±0.10	GL92
——	B1V	26330	4.21	···	8.54 ±0.05	7.64 ±0.05	CL94
AV 304	B0	27500	3.80	14	8.2 ±0.2	6.7 ±0.2	R+02
HD 34078	O9.5V	33000[a]	4.07	20[b]	8.34 ±0.25	7.25 ±0.09	GL92
NGC 346-637	B0V	30500	4.00	28	8.0 ±0.2	$\leq$ 7.2	R+93

Note. — The atmospheric parameters listed here were adopted from ATLAS9 models and spectral syntheses. Solar metallicity was used for HD 36591 and HD 34078, while [Fe/H]=−1.0 models were used for SMC stars. The parameters from GL92 were adopted for HD 36591, with $T_{\rm eff}$ lowered by 3.4%. The O and N abundances have been adjusted to this lower $T_{\rm eff}$ scale (see Δ in Table 9 of GL92), and corrected for the use of Gold NTLE models rather than Kurucz (see Venn *et al.* 2001 for a full discussion). GL92 = Gies & Lambert (1992), CL94 = Cunha & Lambert (1994), R+02 = Rolleston *et al.* (2002), R+93 = Rolleston *et al.* (1993).

[a]Temperature was raised to 33,000 K from the GL92 corrected value of 30352 K, because we expect that HD 34078 should have near solar Fe abundances as it is a runaway Orion star.

[b]While GL92 found $v \sin i$ in this star to be 30±3 km s^{-1}, we found that a lower $v \sin i$ of 20 km s^{-1} was required to fit the sharp lines in this spectrum.

Table 2. HST STIS Observing Information for Galactic B-stars

Star	V	Grat/Slit	Exposure(s)	Date	S/N
AV 304	14.98	G230M	19950 at λ_c2095	26 OCT 99	50
——		52x0.05	+2460 at λ_c2095	29 SEPT 00	
——			+22680 at λ_c2095	all CVZ	
HD 34078	5.96	E230H	432s at λ_c2063	15 MAR 00	55
——		0.1x0.03	+432s at λ_c2013		
HD 36591	5.34	E230M	432s at λ_c2124	09 FEB 99	100
——		0.2x0.05ND	+432s at λ_c2124		
——			+432s at λ_c2124		
——			+434s at λ_c1978		
——			+434s at λ_c1978		
——			+432s at λ_c2269		
——			+432s at λ_c2269		
NGC 346-637	14.98	G230M	2376s at λ_c2095	25 OCT 99	30
——		52x0.05	+12944s at λ_c2095		
——			+2376s at λ_c2095	2 OCT 00	
——			+9708s at λ_c2095		

Table 3. Iron-Group Wavelength Offsets

Elem	λ(KUR)	λ(NEW)	log gf
Mn III	2048.949	2048.918	···
Mn III	2049.357	2049.314	···
Mn III	2049.682	2049.663	···
Mn III	2063.337	2063.397	···
Mn III	2065.886	2065.892[a]	−0.241[a]
Fe III	2050.743	···	0.19
Fe III	2052.271	··· [b]	···
Fe III	2053.524	··· [b]	···
Fe III	2054.492	··· [b]	···
Fe III	2055.863	2055.859	···
Fe III	2056.152	2056.156	···
Fe III	2057.059	2057.072	···
Fe III	2057.928	2057.925	···
Fe III	2058.209	2058.205	···
Fe III	2058.566	··· [b]	···
Fe III	2064.980	··· [b]	···
Fe III	2068.249	2068.263	···
Fe III	2070.539	2070.561	···
Fe III	2070.976	2070.996	···
Fe III	2076.322	2076.318	···
Fe III	2080.220	··· [b]	···
Fe III	2082.384	2082.377	···
Fe III	2084.376	···	0.99
Fe III	2089.093	2089.120	0.28
Fe III	2093.505	2093.512	···
Fe III	2096.426	2096.417	···
Fe III	2099.226	··· [b]	···
Fe III	2100.966	2100.950	0.04
Fe III	2107.322	2107.339	···
Fe III	2108.679	2108.684	···
Fe III	2116.593	2116.583	0.24

[a]Proffit *et al.* (1999)

[b]Changed to E93, then shifted back to Kurucz. Kept E93 gf values.

Table 4. Boron Abundances from STIS Spectroscopy

Star	RV	$\xi_{\rm macro}$	ξ	12+log(B/H)		*12+log(Mn III)*
	($\rm km\,s^{-1}$)			LTE	NLTE	*λ2065.9*
HD 36591	29	18	2	≤1.36	≤1.27	*5.31*
AV 304	145	30	3	≤1.7	≤1.6	*4.9*
HD 34078	56	7	3	≤2.4	≤2.5	*5.4*
NGC 346-637	254	30	2	≤1.5	≤1.6	*4.6*

Note. — Abundances have been determined from spectrum syntheses using the model atmosphere parameters listed here and in Table 1. Radial velocities, ξ, and $\xi_{\rm macro}$ values are determined from the iron-group features. Radial velocities (RV) have been corrected for vacuum-to-air wavelength offsets. NLTE corrections are from calculations in Venn *et al.* (2001). The B III λ2065.8 and Mn III λ2065.9 abundances were varied together in order to achieve the best fit, thus we report the best fit Mn III abundance here in italics.

Table 5. Iron-group Abundance Results

λ (Å)	Element(s)	$[M/H]$ 36591	$[M/H]$ AV304	$[M/H]$ NGC
2048.92	Mn III	−0.09	−0.6	···
2049.37	Fe III+Mn III	−0.10	···	−0.4
2049.66	Mn III	0.00	···	···
2050.74	Fe III	fixed	*1.4*	0.93
2051.85	Fe III+Fe IV	+0.05	···	···
2052.27	Fe III	−0.09	···	···
2053.52	Fe III	−0.24	···	···
2054.56	Fe IIIx3	−0.08	···	···
2055.86	Fe III	*+0.19*	···	···
2056.16	Fe III	+0.08	−0.3	···
2057.07	Fe III	−0.08	−0.4	−1.3
2057.93	Fe III	−0.15	···	−1.0
2058.21	Fe III	−0.03	···	···
2058.57	Fe III	*+0.23*	−0.8	···
2059.67	Fe III	+0.11	*−1.3*	···
2063.40	Mn III	−0.13	···	···
2066.40	Mn IIIx2+Ni III	−0.25	−0.5	···
2068.26	Fe III	*+0.26*	−0.2	−1.4
2068.99	Fe III+Mn III+Cr III	−0.25	−0.9	···
2069.82	Fe III+Mn III	0.00	···	···
2070.56	Fe III	*+0.32*	*−1.2*	−1.0
2070.98	Fe IIIx3	*−0.35*	*0.0*	···
2073.35	Fe III+Mn III	−0.05	···	···
2074.23	Fe III	−0.02	···	*+0.4*
2076.32	Fe III	*−0.54*	···	···
2077.36	Mn III+Co III	−0.05	···	···
2077.74	Fe III+Fe IV	*+0.22*	···	···

Table 5—Continued

λ (Å)	Element(s)	$[M/\mathrm{H}]$ 36591	$[M/\mathrm{H}]$ AV304	$[M/\mathrm{H}]$ NGC
2078.08	Fe III+Mn III	*−0.35*	···	···
2079.00	Fe IIIx4	*+0.20*	−0.7	···
2080.22	Fe III	−0.07	*+0.2*	···
2081.08	Mn IIIx2+Co III	−0.02	···	···
2082.38	Fe III	−0.13	···	···
2083.55	Fe III	+0.09	···	···
2084.36	Fe IIIx3+Mn IIIx2	fixed	+1.3	*2.03*
2084.93	Fe IIIx2	−0.05	−0.8	···
2085.84	Fe III+Cr III	+0.08	···	···
2087.15	Fe III	*+0.16*	···	···
2087.93	Fe III	−0.16	−0.6	···
2089.12	Fe III	fixed	0.9	···
2090.16	Fe IIIx4+Mn IIIx3	0.00	*−1.3*	···
2091.35	Fe IIIx2	*−0.40*	−1.0	···
2092.97	Fe III	0.00	···	−0.8
2093.51	Fe III	−0.08	···	···
2095.66	Fe IIIx3	−0.10	−0.3	···
2096.42	Fe III	+0.13	···	···
2099.30	Fe IIIx2	−0.22	−1.0	···
2101.04	Fe III+Mn III	fixed	0.7	0.83
2103.74	Fe IIIx4	*−0.40*	*−1.5*	···
2104.96	Fe IIIx2+Cr III+Ni III	+0.02	−0.3	···
2105.59	Ni III	−0.13	···	···
2107.34	Fe III	+0.11	−0.7	*−1.7*
2108.64	Fe III+Mn III	−0.15	−0.5	···

Table 5—Continued

λ (Å)	Element(s)	$[M/\mathrm{H}]$ 36591	$[M/\mathrm{H}]$ AV304	$[M/\mathrm{H}]$ NGC
2111.80	Fe IIIx2	*−0.43*	···	···
2113.34	Fe IIIx2+Mn III	−0.25	···	···
2113.83	Fe IIIx2+Cr III	−0.20	−0.6	−1.1
2114.34	Fe IIIx2+Cr III	−0.23	···	···
2114.88	Cr IIIx2	*+0.30*	−0.3	···
2116.59	Fe IIIx2	fixed	*1.4*	···
2117.55	Cr III	*+0.18*	−0.4	···
2118.49	Fe IIIx2+Cr III	*+0.15*	−0.7	···
2120.77	Fe IIIx4+Fe IV	−0.10	···	···
2123.59	Fe IIIx3+Cr III	−0.07	−0.4	···
2124.16	Fe IIIx5+Co III	*−0.47*	···	···
2125.18	Fe IIIx5+Fe IV+Mn III	*−0.30*	−0.4	···
2126.14	Mn III	−0.15	···	···
2129.68	Fe IIIx3	−0.15	···	···
2134.83	Fe IIIx2	*+0.40*	−0.4	···
2136.36	Fe IIIx2	*−0.60*	−0.9	···
AVG		−0.07	−0.6	−1.0
1 σ		0.10	0.2	0.3

Note. — Results are relative to solar abundances in Grevesse & Sauval (1998), e.g., 12+log(Fe/H)=7.50, 12+log(Mn/H)=5.53. Abundances are determined from spectrum syntheses using the parameters listed in Tables 1 and 4. Dominant features only are identified. Results that are $\geq 2\,\sigma$ from the mean are noted in italics and not included in the average. The five lines that have had their oscillator strengths adjusted based on the spectrum of HD 36591 are listed as "fixed" and used *only* in the differential analyses (i.e., not included in the averages listed here).

Table 6. Boron Abundance Uncertainties

	AV 304 $\Delta\log(B/\mathrm{H})$	HD 34078 $\Delta\log(B/\mathrm{H})$	HD 36591 $\Delta\log(B/\mathrm{H})$	NGC 346-637 $\Delta\log(B/\mathrm{H})$
$\Delta T_{\rm eff} = \pm 750$ K	± 0.1	± 0.2	± 0.03	± 0.2
$\Delta\log$ g$= \pm 0.1$	± 0.0	∓ 0.1	± 0.04	± 0.0
$\Delta\xi_{\rm micro} = \pm 1$ km s^{-1}	∓ 0.0	± 0.0	± 0.00	± 0.0
$\Delta\xi_{\rm macro} = \pm 2$ km s^{-1}	± 0.0	± 0.0	± 0.00	± 0.0
Shift Continuum $\pm 2\%$	∓ 0.1	∓ 0.2	∓ 0.12	∓ 0.2
^{11}B $= 2.5\,^{10}$B	0.0	0.0	-0.04	0.0
ΔV$_{\rm rad} = \pm 4$ km s^{-1}	± 0.0	± 0.0	± 0.14	± 0.0
(ΔV$_{\rm rad}$ Mn IIIλ2065.9)*	$\cdots$	($\pm$*0.0*)	($\mp$*0.09*)	$\cdots$

Note. — $\Delta\log$(B/H) was determined by setting Mn III λ2065.9 *a priori* to the best fit (listed in italics in Table 4). We expect the uncertainties in $v \sin i$ to be reflected in $\Delta\xi_{\rm macro}$. For HD 36591 and HD 34078, the uncertainties in continuum placement and radial velocity are half of what is listed here; e.g. the uncertainty in HD 36591 is 1% and 2 km s^{-1}, yielding $\Delta\log(B/\mathrm{H}) = 0.06$ and 0.07, respectively.

*Changing the radial velocity required a completely new fit, i.e. letting B III and Mn III both vary. The new "best" Mn III 2065.9 Å abundance when radial velocity is varied is listed here in italics for this parameter.

Table 7. Present & Local Galactic Boron Abundances

Object	12+log(B/H)	Reference
Solar	2.8	Cunha & Smith 1999
—		Zhai & Shaw 1994
—		Anders & Grevesse 1989
Nebulae	$\geq$2.4	Howk *et al.* 2000
B-stars	2.7	Cunha *et al.* 1997
—	2.4	Proffitt *et al.* 1999
—	2.3	Proffitt & Quigley 2001
—	2.4	Venn *et al.* 2001
FG-stars	2.6	Cunha *et al.* 2000a
—	2.5	Cunha *et al.* 2000b
	2.5	ADOPTED

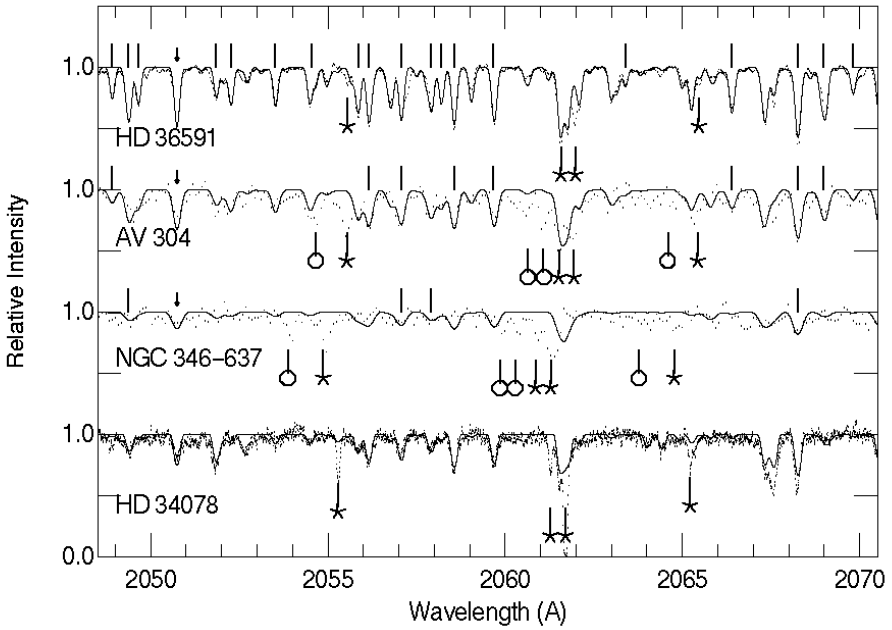

Fig. 1.— Coadded HST STIS spectra for SMC (AV 304 and NGC 346-637) and Galactic (HD 36591 and HD 34078) stars (*dotted line*) and their spectrum syntheses (*thin line*). The iron-group metallicities in Table 5 were used for each synthesis, i.e., $[M/\mathrm{H}]$=0.07, −0.6, and −1.0 for HD 36591, AV 304, and NGC 346-637, respectively. Solar iron-group abundances are adopted for HD 34078 (see text). All features listed in Table 5 are identified by a line *above* the feature; features used solely for a differential analysis are marked by an arrow. Interstellar lines are marked *beneath* the spectra. Note that the SMC stars have two sets of IS lines (represented by different symbols). The Galactic spectra were smoothed for a 3 pixel resolution element.

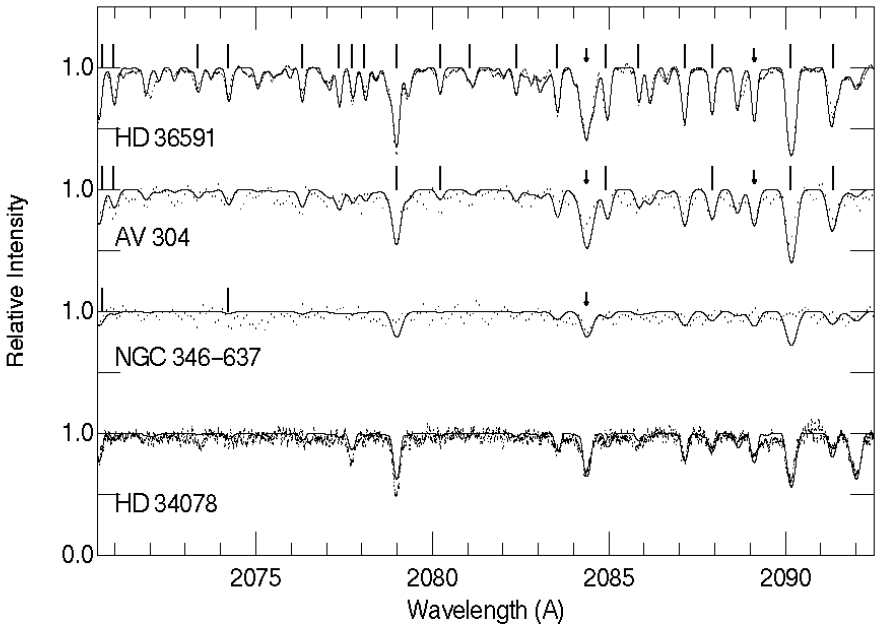

Fig. 2.— See comments in Figure 1.

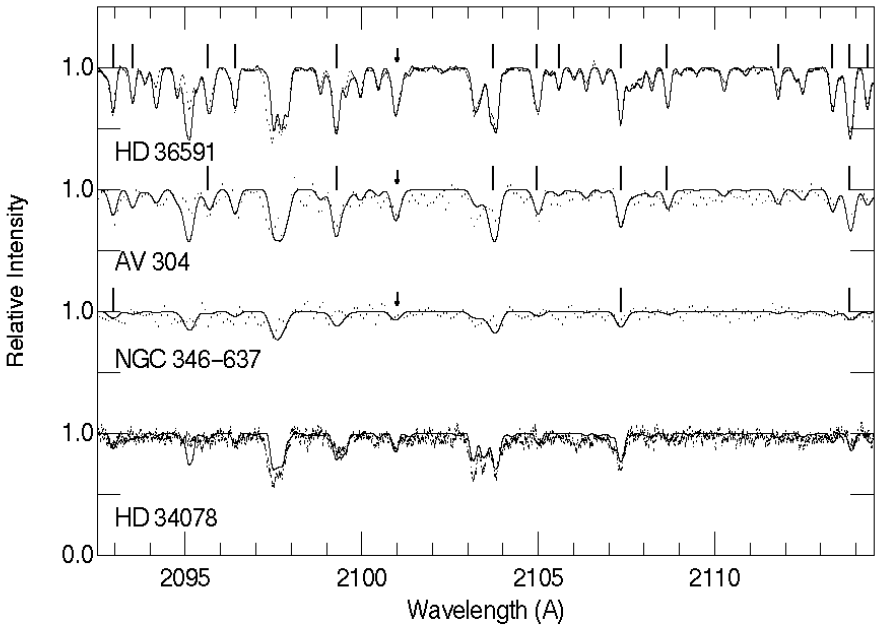

Fig. 3.— See comments in Figure 1.

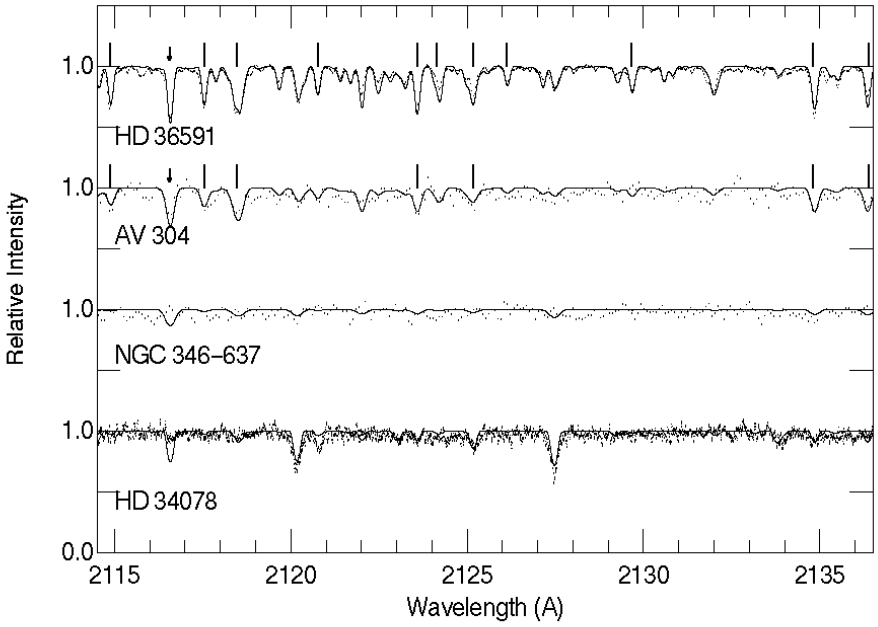

Fig. 4.— See comments in Figure 1.

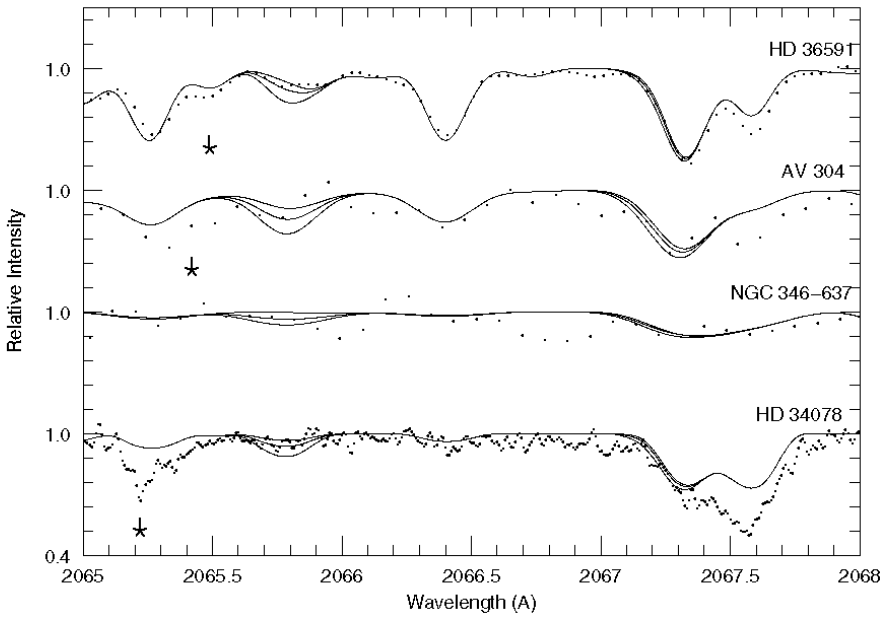

Fig. 5.— Boron syntheses for all program stars. The best fit syntheses are shown, as well as $\Delta\log(\mathrm{B/H})=\pm0.3$ for comparison, except for NGC 346-637 where the best fit, +0.3, and no boron ($12+\log(\mathrm{B/H})=-10$) are shown. Interstellar lines are again noted. The spectra of HD 36591 and HD 34078 are shown in Venn *et al.* (2001) for the same wavelength region, but the spectra here are synthesized at different temperatures (HD 36591 has been lowered 3.4% and HD 34078 has been raised to 33,000 K, see text).

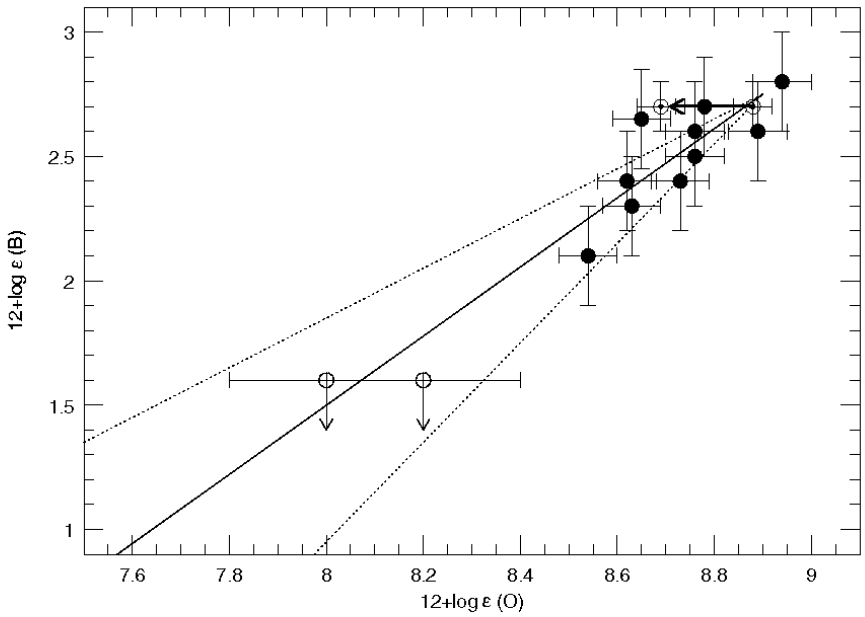

Fig. 6.— Galactic disk stars' boron and oxygen relationship from Smith *et al.* (2001; *solid circles*). In this log-log plot of abundances, the relationship has slope of 1.39 ±0.08 (*solid line*), or N(B) is proportional to $N(O)^{1.4}$. A new solar abundance by Allende-Prieto, Lambert, & Asplund (2001) of 12+log(O/H)=8.69 ±0.05 is noted, and would change the slope slightly to 1.5. Also shown are the predictions for a linear (slope of 1.0) and quadratic (steeper slope of 2.0) relationship between boron and oxygen. We note that the two SMC B-star upper-limit abundances (*open circles*) are in good agreement with the Galactic disk slope. However, the linear relationship cannot be ruled out if boron has been depleted by rotational mixing.